

## Weathering and River Erosion: Insights from the Variation of Intact Rock Strength in Rhyodacites

*Intemperismo e Erosão Fluvial: Insights a Partir da Variação da Resistência da Rocha Intacta em Riodacitos*

Adalto Gonçalves Lima<sup>1</sup> , Ana Carolina Carvalho Galvão<sup>1</sup>  & Diego Moraes Flores<sup>2</sup> 

<sup>1</sup>Universidade Estadual do Centro-Oeste, Departamento de Geografia, Guarapuava, PR, Brasil

<sup>2</sup>Universidade Federal da Integração Latino-Americana, Instituto Latino-Americano de Tecnologia, Infraestrutura e Território, Foz do Iguaçu, PR, Brasil

E-mails: [adalto@unicentro.br](mailto:adalto@unicentro.br); [anacarolinacgalvao@gmail.com](mailto:anacarolinacgalvao@gmail.com); [diego.flores@unila.edu.br](mailto:diego.flores@unila.edu.br)

**Corresponding author:** Adalto Gonçalves Lima; [adalto@unicentro.br](mailto:adalto@unicentro.br)

### Abstract

The relationship between weathering and fluvial erosion is important in shaping the incisions of bedrock channels. In rhyodacites from Paraná Volcanic Province, plucking and macro-abrasion processes are predominant in the fluvial incision process, according to field observations. Using the intact rock strength as a proxy for the weathering, this paper analyzes how the strength of rhyodacites behave along a cross section of a bedrock channel and seeks to understand how this affects erosion. Topography and intact rock strength were surveyed continuously along a 30 m cross section using a Schmidt hammer, model N. Mean, median, and standard deviation were calculated for each meter of the section. The topographic amplitude of the bed in the section is 30 cm, featuring an almost flat geometry. The average strength values range from 30 to 59 R (7.65 to 58.15 MPa). Despite the small topographical amplitude, the general behavior of the rock strength follows the macrotopography of the bed, increasing in the high zones and decreasing in the low zones. The standard deviation, interpreted as directly proportional to the degree of weathering, follows the microtopography of the bed (amplitude  $\approx 10$  cm), being greater in low areas and smaller in high areas. This association between standard deviation of strength and microtopography reveals the seasonal variation of the water level in the channel, whereby higher moisture in low-lying areas intensifies the weathering of the rock. Weathering affects the density of rhyodacites in the area with a minimum reduction of 11.2% being calculated. This enhances the erosion processes by plucking and macroabrasion by reducing the intact rock strength. The susceptibility of the rhyodacites to weathering, despite the differences within the section, favors the maintenance of the rectangular geometry of the channel and shows how erosive processes are affected by the condition of the rock. The study revealed that the notion of decreasing the intact rock strength towards the banks associated with greater weathering in higher areas, cannot be generalized, as it depends on the geometry of the channel section, the lithological nature of the bed, and the frequency of flows.

**Keywords:** Bedrock river; Rhyodacite; Erosion resistance

### Resumo

A relação entre intemperismo e erosão fluvial é importante para configurar a incisão dos canais rochosos. Em riodacitos da Província Paraná processos de arrancamento e macroabrasão são predominantes no processo de incisão fluvial e seu controle pelo intemperismo é sugerido pelas observações de campo. Utilizando a resistência da rocha intacta como proxy para o intemperismo, este artigo analisa como a resistência dos riodacitos se comporta ao longo de uma seção transversal de um canal rochoso e busca entender como isso afeta os processos erosivos. Uma seção transversal de 30 m de comprimento foi levantada topograficamente e a resistência da rocha foi medida de modo contínuo ao longo dela, utilizando-se um esclerômetro modelo N. Média, mediana e desvio padrão foram calculados a cada metro da seção. A amplitude topográfica do leito na seção é de 30 cm, caracterizando uma geometria quase plana. Os valores médios de resistência variam de 30 a 59 R (7,65 a 58,15 MPa). Apesar da pequena amplitude topográfica, o comportamento geral da resistência média da rocha acompanha a macrotopografia do leito, aumentando nas zonas altas e diminuindo nas zonas baixas. O desvio padrão da resistência, interpretado como diretamente proporcional ao grau de intemperismo, acompanha a microtopografia do leito (amplitude  $\approx 10$  cm), sendo maior nas zonas baixas e menor nas zonas altas. Essa associação entre desvio padrão da resistência

e microtopografia revela a variação sazonal do nível da água no canal, pela qual a maior umidade em zonas baixas intensifica o intemperismo da rocha. O intemperismo afeta a densidade dos riodacitos da área, sendo calculada uma redução mínima de 11,2%. Isto potencializa os processos de erosão por arrancamento e por macroabrasão, porque diminui a resistência da rocha. A suscetibilidade dos riodacitos ao intemperismo, a despeito das diferenças internas à seção, favorece a manutenção da geometria retangular do canal e mostra a subordinação dos processos erosivos a essa condição da rocha. O estudo revelou que o conceito de diminuição da resistência da rocha intacta em direção às margens, associado ao maior intemperismo em zonas mais elevadas, não pode ser generalizado, pois depende da geometria da seção do canal, da natureza litológica do leito e da frequência dos fluxos.

**Palavras-chave:** Rio de leito rochoso; Riodacito; Resistência à erosão

## 1 Introduction

Unlike alluvial rivers, which cut through their own previously deposited sediment, bedrock river erosion is primarily responsible for the evolution of the landscape, as it commands the rates of reduction in base levels (Whipple, Dibiase & Crosby 2013). As a result, the study of incision in bedrock channels is the focus of models that seek to understand the evolution of the landscape (e.g., Attal et al. 2008; Langston & Tucker 2018). Underlying these studies is the need to understand how rivers operate as a function of climatic (e.g., Ferrier, Huppert & Perron 2013), tectonic (e.g., Whittaker et al. 2007), and rocky substrate (e.g., Small et al. 2015).

The erosion processes that operate in bedrock rivers depend on the relationship between hydraulic aspects (stream power and shear stress) and the rock characteristics, that is, the strength of the intact rock (without fractures) and the presence of discontinuities (joints and bedding planes). Heavily fractured rocks, such as basalts, tend to favor plucking erosion (Hancock, Anderson & Whipple 1998; Lima & Binda 2013) while more massive rocks favor abrasion erosion (Sklar & Dietrich 2001; Stock et al. 2005). The rhyodacites, which layer the Paraná-Etendeka Volcanic Province (Jerram & Widdowson 2005), have a low density of syngenetic fractures, which increases the intact rock strength and makes it more resistant to fluvial erosion. However, the presence of abrasive features – such as potholes, furrows, and shell marks – is not common in riverbeds in these rocks. Field observations suggest that the chemical/physical weathering process of rhyodacites facilitates macroabrasion and even the plucking of large sections of rock, by decreasing the rock strength (Flores, Lima & Oliveira 2018).

The effects of weathering on erosive processes of abrasion and plucking are notorious, either by reducing the strength of rocks or by widening fractures (Hancock, Anderson & Whipple 1998; Whipple, Hancock & Anderson

2000). However, weathering can vary spatially within the same channel. In a cross-section, weathering varies mainly as a function of water level oscillation, accounting for differences in the intensity of intracanal erosion (Murphy et al. 2016; Shobe et al. 2017; Small et al. 2015). The relationship between weathering and river erosion is an important component in understanding how the geometry of rock channels evolve (Hancock, Small & Wobus 2011). However, the relationship between weathering and the specific dynamics of each erosive process still needs to be better understood. The study of beds in rhyodacites can improve the understanding of the relationship between weathering, plucking, and macroabrasion processes. In addition, rhyodacites, and associated felsic rocks, cap large continental basaltic flows, such as that of the Paraná-Etendeka Province (Jerram & Widdowson 2005; Nardy, Machado & Oliveira 2008), occupying considerable areas. Their geomorphological behavior is important for the evolving landscape of these geological provinces. So far, little is known about how the fluvial incision occurs in these rocks, constituting a great gap in the geomorphological knowledge of these regions of the Earth.

In this study, using data from a Schmidt hammer, we analyzed in detail the strength of rhyodacites in a 30 m cross section of a river, considering strength as a proxy for weathering. Unlike other studies (e.g., Murphy et al. 2016; Shobe et al. 2017; Small et al. 2015), which sampled the strength of more incised fluvial channels, here we analyze a rectangular channel with a greater widening tendency than deepening. The continuous strength survey, following the entire topography of the bed, made it possible to verify the variability of rock conditions and erosion along the section and revealed new details about the variation of weathering in the bedrock channels. Alongside the quantification of the strength and topography of the bed, observations of field features helped to build a conceptual model for erosion in this type of riverbed.

## 2 Study Area

The study area is on felsic rocks of the Paraná Volcanic Province, southern Brazil (Figure 1). This province is associated with the continental breakup between South America and Africa and the consequent opening of the Atlantic Ocean (Peate 1997), dating from 137 to 127 Ma

(Turner et al. 1994). Felsic rocks constitute the top of the volcanic sequence and appear on both the Brazilian and African sides (Jerram & Widowson 2005; Marsh et al. 2001), representing about 10% of the province (Piccirillo et al. 1988). The Guarapuava plateau, on which the study area is located, is formed by felsic volcanic rocks of the Chapecó type (Bellieni et al. 1986). These rocks are porphyritic,



**Figure 1** Study area: A. Localization map; B. Cross section site.

with plagioclase phenocrystals (up to 2 cm) immersed in a light gray aphanitic matrix composed of augite, pigeonite, magnetite, and apatite, in addition to quartz and feldspar (Nardy, Machado & Oliveira 2008). The characteristic structure of these outcropping rocks is the igneous banding. When weathered, the rhyodacites in the area take on a yellowish color, with the plagioclase phenocrysts being completely dissolved, leaving their molds empty on the exposed surfaces.

The bodies of rhyodacite are generally tabular, horizontal and extend for several kilometers. On the eastern edge of the Guarapuava plateau, the maximum outcrop thickness of this unit is approximately 50 m (Lima 2020). The systematic occurrence of sub-horizontal joints ( $<10^\circ$ ), associated with strongly inclined joints ( $>30^\circ$ ) found in an outcrop located about 500 m northeast of the area, suggest the existence of a wavy structure, perhaps a dome. Sub-horizontal joints in the riverbed reinforce this interpretation.

The area selected for the study is in the Coutinho River, in the municipality of Guarapuava, state of Paraná. This river is a tributary of the Jordão River, which is one of the main tributaries on the right bank of the Iguçu River (Figure 1). The Coutinho river basin has an area of 601 km<sup>2</sup>, and the upstream part of the analyzed reach is equivalent to 161 km<sup>2</sup>. The studied reach constitutes a continuous bedrock segment, approximately 160 m long and 30 m wide. The river reach morphology is stepped, with an average slope of 0.025 m/m. This is the only significant bedrock reach found in Coutinho. In the upstream segment of the area, the bed is predominantly alluvial, and the channel has a tortuous to meandering pattern.

The climate of the region is temperate, due to high altitudes ( $>1000$  m), with average annual temperatures ranging between 16° C and 20° C, and frosts are common during winter ( $\approx 12$  events; Thomaz & Vestena 2003). Rainfall is well distributed throughout the year and annual totals are around 1800 mm (Paraná 1998). Precipitation in the region is also conditioned by the El Niño and La Niña events, which have a direct influence on the minimum and maximum flows of rivers. During El Niño, rainfall is abundant and responsible for positive anomalies while during La Niña there are long periods of drought (Grimm, Ferraz & Gomes 1998).

### 3 Methodology and Data

The bedrock reach of the Coutinho River was chosen for this study due to some characteristics. The most important is the exposure of the bedrock for more than 100 m, allowing the observation of various details of the rock weathering and erosion. Another feature is that it

is located downstream of a small dam ( $\approx 2$  m high), built to divert water to an industry, which leaves the bed with many exposed areas during low winter flows. This was the case during the research field survey.

A cross section of the channel was selected with a width of 30 m and distance of about 70 m from the dam while being totally free of loose blocks or sparse sediment accumulations (Figure 2). Across the section, the slope of the channel was obtained, using laser leveling and a ruler in a stretch of 18 m. Along the section, the topographic profile and the bedrock strengths were surveyed. The topographic profile was obtained using a ruler and a laser distance meter (Leica Disto A5) mounted and leveled on a tripod. The strengths were measured with a Schmidt hammer, model N (Proceq N34).

Along the chosen section, strength measurements were obtained continuously. Around 15 to 30 measurements (Niedzielski, Migon & Placek 2009) were taken at each meter of the section, randomly distributed in a strip of approximately 50 cm width (Figure 2). Following the recommendations of the literature (Aydin & Basu 2005; Day 1980; Sumner & Nel 2002) in order not to dissipate the impact energy of the rebound hammer, measurements close to joints ( $<10$  cm) and on surfaces covered with moss or water were avoided. In the rhyodacites of the studied area, weathering is common, producing exfoliation in the bed. Many of these slabs, when thin ( $<5$  cm), produce abnormally low values of strength when impacted by the Schmidt hammer, due to the millimetric gap with the bed in its edge region. Such areas were avoided in the survey of measures. In the riverbed, only relatively horizontal surfaces were evaluated, and it was not necessary to normalize the values obtained by the Schmidt hammer (Basu & Aydin 2004).

The data obtained with the Schmidt hammer were statistically treated to obtain the mean, median, and standard deviation for each meter of the cross section. Although the mean is the most used parameter, it may not be consistent. This is because rock strength can vary over a small area due to uneven weathering and generate outliers that make the mean not the central measure of the distribution. The median, on the other hand, tends to return a more realistic characterization in these cases of outliers.

The Schmidt hammer assesses the strength of the rock against the impact of a steel pointer and records the rebound values on a proper scale (R). These values can be correlated with uniaxial compressive strength, as shown by several studies (see references in Aydin & Basu 2005; Dinçer et al. 2004; Yagiz 2009). For this research, the final averages of R were converted according to the empirical formulation of Aydin and Basu (2005) obtained for granitic rocks with different degrees of weathering (Equation 1).



**Figure 2** Cross section analyzed in the study (dashed line), with a 50 cm width strip where the strength measurements were obtained.

$$UCS = 1.45 e^{(0.07R)} \quad (1)$$

where UCS is the uniaxial compressive strength (MPa) and R is the rebound value of the Schmidt hammer.

## 4 Results

### 4.1 Rock Characteristics

In the studied reach, mainly in the analyzed section (Figure 2), the rhyodacites have sparse vertical joints. A conjugate system of tectonic joints is present in the section (Figure 3A). These joints are responsible for the direction of the flow at low discharges, due to the ease of erosion in these zones of pervasive discontinuity of the rock. Horizontal to sub-horizontal joints are more common in the analyzed bed and form broader planes inside the rock mass, facilitating water percolation and, consequently, weathering (Figure 3B). With this, rock slabs are generated in the bed, with thicknesses varying between 5 and 30 cm. The mineralogical discontinuities, visible in the banding of

fresh rhyodacite, respond differently to chemical weathering and are responsible for the generation of thinner slabs.

Along the analyzed section, it is possible to observe, mainly in the left half, sub-horizontal joints whose planes follow the slope of the bed and produce steps contrary to the flow direction (Figure 3C). These joints form plates with thicknesses of a few centimeters, with more accentuated weathering in the area close to the step and progressively decreasing in the reverse. Throughout the upstream and downstream of the section, the sub-horizontal joints appear conspicuously and reveal an inclined structure, probably dome-shaped, relatively common in the rhyodacites of the region.

Chemical weathering of rhyodacites occurs primarily by the destruction of plagioclase phenocrysts, which are replaced by clay minerals that modify their color (Truffi & Clemente 2002). With the removal of the replacement minerals, only cavities with the shape of the previous plagioclase crystals remain. The matrix, formed by a quartz-feldspathic fabric, oxides, and hypohyaline bands, weathers afterwards, generating a progressively more porous and yellowish material.



**Figure 3** Fractures present in the study area: A. Set of vertical joints, visible on the right side of the channel; B. Horizontal joints located downstream of section; C. Sub-horizontal joints located on the left side of the section.

### 4.2 Cross Section Profile

In the studied cross section (Figure 4), the right bank of the channel is rocky and the level of mosses and lichens, as well as the shrubby vegetation, mark the level of the bankfull margins at a height of approximately 0.8 m. The left bank is formed by an island, which rises over the bed at an approximate height of 0.5 m. The island is a bar of sediment, on which dense arboreal vegetation develops. The maximum difference in height of the topographic features of the bed is approximately 40 cm. However, if only the bed on which the strength measurements were taken is considered, this difference in height is 30 cm. This gives the channel an almost flat bed characteristic.

Despite the small topographical variation, the section profile reveals a deeper and asymmetrical zone towards the right margin, separated from another deep and symmetrical zone by an elevation in the bed. The deepening of the channel along the left bank is just an area excavated by

plucking, with no downstream exit. In this text, this general morphology is called macrotopography, to differentiate it from microtopography, formed by small unevenness (amplitude  $\approx 10$  cm) of eroded blocks.

### 4.3 Intact Rock Strength

Along the cross section, the average strength varies from 30 to 59 R, not continuously, but following the macrotopography of the bed (Figure 5). The lowest values ( $< 40$  R) occur in the lowest areas of the bed, while the highest values ( $> 40$  R) tend to be concentrated in the relatively higher areas. Based on equation (1), the mean values of R were converted to uniaxial compressive strength (Table 1). Values range from 7.65 to 58.15 MPa. However, despite the sequential trends being the same as noted for the values of R, it is notable that the strengths are concentrated between 10 and 30 MPa.

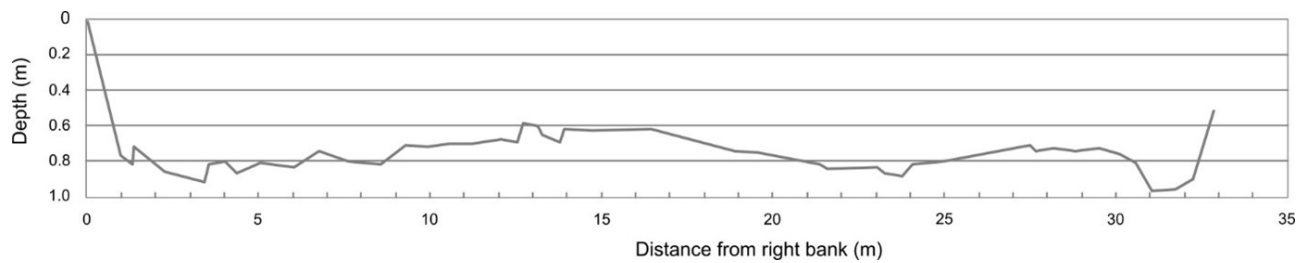


Figure 4 Profile of the studied cross-section, looking upstream. Depth from bankfull level.

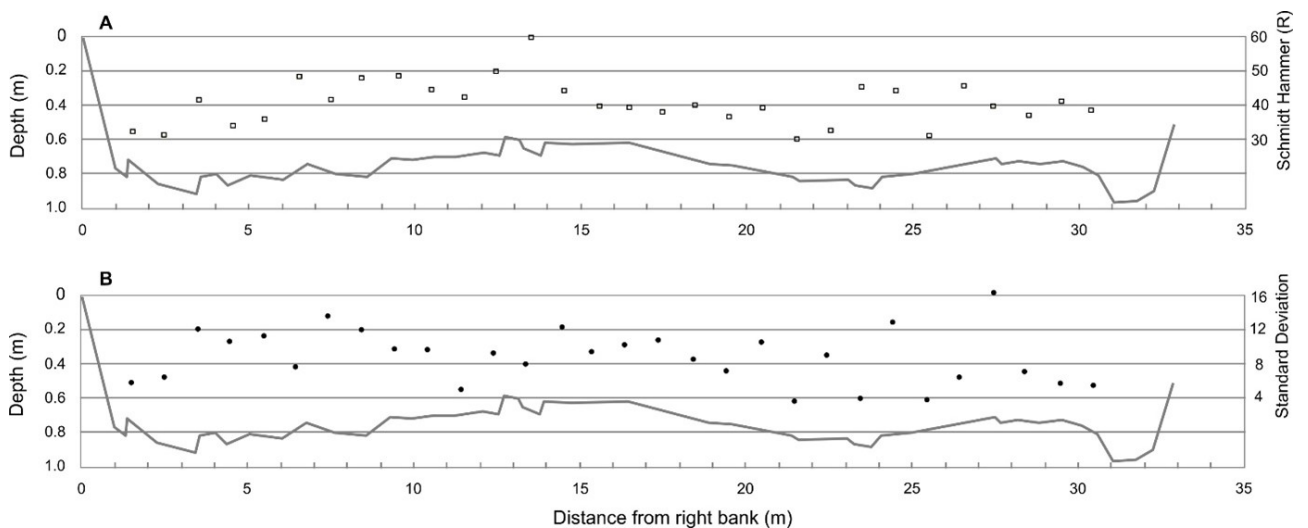


Figure 5 Cross-section profile with plot of: A. Mean strength/meter, measured with a Schmidt hammer; B. Standard deviation of measures.

Along each sampled meter, here called the sampling zone, the average variability of the strength measured with a Schmidt hammer is 10 R, with a minimum equal to 6 and a maximum 16. The average and median do not differ much from each other in each of the zones sampled (Table 1). In only two zones this difference is 4 R, while in the others the difference is around 1 R. The distribution of standard deviations of R along the section shows some trends (Figure 5). At first sight when analyzing the stratification of values, it

is noted that there is a greater concentration of low values of deviation ( $< 9$  R) on the left side of the channel, although the differences between one zone and another are the largest in the section. Analyzing the trends in deviations in contiguous zones, starting from the right side of the channel, we notice three segments repeating a pattern of progressive decrease in deviations. This repetitive pattern encompasses more than half of the section. On the left side, the pattern is one of alternating between very distinct high and low values.

**Table 1** Statistics of strength data in the cross section.

Sample zone	R	SD	Var	UCS MPa	Dens. G/cm <sup>3</sup>
1	32.3	7.5	32	8.8	2.25
2	31.3	8.0	30	8.2	2.24
3	41.7	12.4	46	17.0	2.34
4	34.1	11.3	33	10.0	2.27
5	36.0	11.7	35	11.4	2.29
6	47.3	8.9	48	25.2	2.40
7	42.3	13.6	40	17.7	2.35
8	47.8	12.4	48	26.1	2.40
9	48.2	10.5	48	26.9	2.40
10	45.5	10.6	46	22.2	2.38
11	42.6	7.0	43	18.2	2.35
12	49.6	10.2	50	29.6	2.42
13	59.2	9.1	62	58.1	2.51
14	44.9	12.5	48	21.3	2.37
15	40.6	10.3	42	15.7	2.33
16	39.0	11.0	39	14.1	2.32
17	38.0	11.4	39	13.2	2.31
18	39.7	9.6	40	14.8	2.32
19	36.5	8.8	36	11.9	2.29
20	39.0	11.3	40	14.1	2.32
21	30.3	5.8	30	7.7	2.23
22	33.1	10.1	34	9.3	2.26
23	45.9	6.2	46	22.9	2.38
24	45.3	13.0	46	22.0	2.38
25	31.6	6.0	32	8.4	2.25
26	46.6	8.1	48	24.0	2.39
27	40.0	15.7	38	15.1	2.33
28	36.4	8.6	37	11.8	2.29
29	41.1	7.5	44	16.3	2.34
30	37.4	7.2	38	12.6	2.30

**R:** Schmidt Hammer rebound value; **SD:** standard deviation; **Var:** variance; **UCS:** Uniaxial Compressive Strength; **Dens.:** density.

## 5 Discussion

### 5.1 Strength and Weathering

The uniaxial compressive strength of the rhyodacites in the section (Table 1) was calculated based on the empirical relationship with the Schmidt values obtained by Aydin and Basu (2005) in granites. The use of this relationship took place considering the petrography and chemistry of rhyodacites as being close to the granites. According to Aydin and Basu (2005) and Yagiz (2009), it is unlikely that there is a universal relationship between the values of R and the UCS for all lithologies. This makes the values obtained for this study to be considered with some caution and reinforces the use of the rebound hammer as an efficient method to comparatively measure the resistance of rocks in the field.

Despite the restrictions, the relatively low UCS values for rhyodacites can reveal, in general, a low strength of the intact rock, a characteristic of highly weathered igneous materials. This is supported by field observations, which point to the rapid and ubiquitous weathering of plagioclase phenocrysts. These crystals make up about 1/3 or more of the volume of rhyodacites. The characteristic weathering process of porphyritic rhyodacites is possibly responsible for two aspects observed in the field data: the variation in strength of each sample zone and the loss of rock density. Both have implications for erosive processes.

Erosion resistance depends on the absolute value of the intact rock strength (Sklar & Dietrich 2001), but in the case of the studied rhyodacites, the analysis of strength variation is an important component. The strength variation in the sample zones is indicated by the standard deviation. Sometimes, areas with the same average strength have different dispersions. Greater dispersion means advancing weathering, which ends up being a heterogeneous process due to differences in the susceptibility of the mineralogical components of rhyodacite (Caner et al. 2014; Truffi & Clemente 2002).

On the right side of the channel, repeated segments of progressive decrease in standard deviations of R stand out (Figure 5). An explanation for this repetitive pattern may be related to the water flow levels of the channel, visible in the microtopography of the section (Figure 5). Each segment would represent the water level oscillation within a seasonal phase, below bankfull. In each phase, the lower the zone of each segment, the longer moisture remains in the rock, due to more frequent flows. This favors chemical weathering, which results in a decrease in rock strength and an increase in its standard deviation (Figure 5). The average strength behavior on the right side of the channel, following

the topography of the bed, reinforces the notion of greater weathering of the rock in the deepest part of the channel.

As the results indicated, there is a predominance of smaller standard deviations ( $< 9 R$ ) on the left side of the channel, while there is an alternation with larger values. Low values indicate segments that have had their weathering layer removed, that is, they are subject to more efficient erosion. High values, in turn, characterize segments in which the weathering layer remains. The juxtaposition of such contrasting situations can be explained by the relationship between the direction of the section and the fractured pattern of the rhyodacites in the area (Figure 3). Higher energy flows, when acting in this zone of the channel, produce erosion that removes more weathered parts of the tabular blocks, exposing less weathered underlying parts. Though less noticeable, the average strength follows this alternating pattern (Figure 5).

The loss of mass due to chemical weathering, mainly of plagioclase, can be translated into a decrease in rock density, as it increases its porosity and reinforces the weathering cycle (Caner et al. 2014). Using the relationship obtained by Aydin and Basu (2005), the density of rhyodacites in the section analyzed was calculated based on the values of R (Table 1). Considering the maximum and minimum densities estimated in the section (2.51 and 2.23 g/cm<sup>3</sup>, respectively), it appears that there is a reduction of 11.2% related to the rock weathering. This is a minimum value, as throughout the entire section the rock it is weathered to a greater or lesser degree. The complete removal of plagioclase phenocrysts, or the advanced stages of their weathering, favor the formation of microcracks in the rock mass. Microcracks can be induced by daily thermal stress and be further explored by other chemical and physical weathering processes (Eppes et al. 2016). Consequently, it increases the potential erodibility of the rock, making it more vulnerable to less intense processes.

### 5.2 Strength and Bed Topography

The sequential survey of the strength of rhyodacites in the cross section, when compared to the topography of the bed (Figure 5A), reveals a different behavior in relation to the conceptual model of other authors (for example, Shobe et al. 2017; Small et al. 2015), which postulates a strength increase towards the thalweg. According to this model, more erosion would occur in the thalweg area, leaving the rock less weathered on the surface. On the other hand, towards the banks, erosion would be less active due to the variation in the water level, which leads to an intermittence in the exposure of the bed, subjecting it more effectively to weathering processes (chemical and physical).

In the studied case, the channel is of the rectangular type, which means an approximately balanced distribution of water along the section, with the most significant level changes being registered only in the vertical wall of the right bank. Despite the rectangular shape, the topography of the bed reveals two gently lowered zones. It would be expected that in these zones the weathering and rock strength would be the same as that theorized for channels with larger incisions. In contrast, in the section studied, strength follows the macrotopography of the bed. The lower zones have less strength and the higher ones, greater strength. Note that the use of the terms high and low is made here by observing the trend of values (Figure 5A).

Lower segments mean greater concentration of flow and erosion. At the right end of the channel, as there is a lowering of the bed, a greater strength of the rock was expected. However, the strength progressively decreases towards the lower zone. The same occurs on the left portion of the channel. This fact, as well as the behavior of the standard deviations that inversely follow the topography of the bed, as discussed earlier (Figure 5), affirm the conclusion that the weathering is more concentrated in the lowered areas.

Due to inadequate exposure conditions, no strength measurements were taken on the channel wall. However, the apparent situation of the rock, with high moisture and cover of mosses and vegetation, denotes a low strength. Thus, it is very likely that the strengths measured in the section are, in fact, greater than in the channel wall, which points to its more continuous erosion state. On the other hand, the relationship between topography-strength identified in the section is probably due to the altimetric interval of the bed in the section ( $\approx 40$  cm) being too small to express the behavior of the channels with larger intervals. The trends noted in the mean and standard deviation of the strengths are consistent and not a fortuitous condition. Therefore, the low bed topography is interrelated with small and varying flows, especially in the winter where more wetting-drying cycles exist, unrelated to the distance from the margin or the thalweg.

### 5.3 Channel Erosion

Erosion occurs across the entire section, probably under bankfull flows or greater (Baker & Kale 1998; Wohl 1998). At the right end of the channel, the topography of the bed is more irregular than in the rest of the section, denoting the more effective action of the plucking process (Figure 3A). The irregularity is defined by the edges of blocks delimited by fractures. Although, macroabrasion appears as an important process in this sector of the channel, in the remainder of the section, the less irregular shape of

the topography reflects the predominance of macroabrasion, which promotes the removal of the most weathered parts of the tabular blocks (Figure 3C).

With the plucking process, areas of the rock delimited by vertical fractures are removed almost entirely and create recessed areas more susceptible to the concentration of water. This makes the wetting-drying cycles more frequent on the right side of the channel, creating a cycle that leads to greater erosion. Wetting-drying cycles have been analyzed in relation to erosion in sedimentary rocks (Johnson & Finnegan, 2015; Montgomery 2004). In the case of rhyodacites, the wetting phase provides the rock with conditions for chemical weathering, while the drying phase favors physical weathering, with the development of microcracks (Eppes et al. 2016).

Erosive processes – whether by plucking or macroabrasion – are facilitated by vertical and horizontal cracks that are generated by the advancement of weathering. As previously described, weathering causes the reduction of rock density and strength, through the chemical removal of minerals and the increasing occurrence of micro-cracks (Caner et al. 2014; Shobe et al. 2017). With this, some pieces of rock are easily extracted, either by macroabrasion or by pure plucking.

The shape of the analyzed section, as well as the entire reach of which it forms part, is rectangular. This shows a trend of widening overlapping with deepening and, as demonstrated by Hancock, Small and Wobus (2011), is indicative of a section where weathering predominates. Field data supports this conclusion while pointing to the variability of erosive conditions in the bed. Both processes identified as acting in the section bed, that is, plucking and macroabrasion, have their effectiveness increased by the weathering of the rhyodacites, turning it into resistance. Despite the differences in processes and intensities derived from the distribution of flux and erosive energy, the shape of the section reveals a long-term equilibrium, which keeps it rectangular. On the one hand, plucking is more effective and produces a localized deepening of the channel, while on the other hand, macroabrasion benefits from the horizontal/sub-horizontal fractures inherent in this type of rock and from the cracks produced by weathering during periods of greater exposure.

The erosive evolution of the bed in the analyzed section can then be summarized in a conceptual model based on strength/weathering data and field observations carried out in the section. In general, weathering differences cause certain areas of the bed to be more eroded than others, causing its topographic lowering. Vertical joints are the most favorable places to start this process. Weathering occurs along the entire bed of the section; once an initial erosive

anisotropy is established, the low areas undergo wetting-drying cycles, or chemical-physical weathering cycles, more frequently than the higher zones. Wetting-drying intermittency may be greater in low-lying areas, due to flows occupying these areas more frequently than higher topographic levels. These flows, associated with autumn and winter, have depths of a few centimeters, facilitating their intermittence and, consequently, the exposure of the bed. Thus, chemical and physical weathering alternate and prepare the rock for erosion in the lower areas. At the same time, horizontal cracks propagate (Eppes et al. 2016; Hancock, Anderson & Whipple 1998) towards higher and less weathered blocks, predisposing them to plucking during more significant flow events. Pervasive horizontal joints, originating from the rock formation process (syngenetic), work in the same way as horizontal cracks propagated by weathering, with the difference being that they isolate thicker tabular blocks that are plucked by extreme events.

## 6 Conclusion

The average strength of the rhyodacites in the cross section of the river with an almost flat geometry, measured with a Schmidt hammer, showed to be between 30 and 59 R, although most of the values (97%) are concentrated between 30 and 50 R. Converted to UCS, these values reveal low material strength, indicating weathering throughout the entire section. Differential weathering is still responsible for the average resistance variation of around 10 R found in each sample zone.

Within the observed rock strength range, there is a reduction of about 11% in rock density in relation to higher and lower resistances. The development of horizontal cracks follows the process of decreasing strength and density. Thus, although experimental data is still lacking, it is possible to expect that this reduction in density may influence the predisposition of the rock to plucking and macroabrasion, which are predominant processes in the studied area.

Along the section, in general, the strength of the rock follows the macrotopography of the bed, which varies a few decimeters, being relatively greater in the high zones and smaller in the low zones. The standard deviation of the strength has an inverse behavior to the bed microtopography (<10 cm). These results, taken together, support the conclusion that weathering is more concentrated in the lower areas, due to the intermittent presence of water related to more frequent flows. Therefore, the theory that decreased intact rock strength towards the banks is a result of greater weathering in higher areas, is not always the case and shouldn't be generalized, as it depends on the geometry of the channel section, the lithological nature of the bed, and the frequency of flows.

## 7 References

- Attal, M., Tucker, G.E., Whittaker, A.C., Cowie, P.A. & Roberts, G.P. 2008, 'Modeling fluvial incision and transient landscape evolution: Influence of dynamic channel adjustment', *Journal of Geophysical Research: Earth Surface*, vol. 113, no. (F3), DOI:10.1029/2007JF000893
- Aydin, A. & Basu, A. 2005, 'The Schmidt hammer in rock material characterization', *Engineering Geology*, vol. 81, no. 1, pp. 1-14, DOI:10.1016/j.enggeo.2005.06.006
- Baker, V.R., & Kale, V.S. 1998, 'The Role of Extreme Floods in Shaping Bedrock Channels', in K.J. Tinkler & E.E. Wohl (eds), *Rivers Over Rock: Fluvial Processes in Bedrock Channels*, American Geophysical Union, Washington DC, pp. 153-64, DOI:10.1029/GM107
- Basu, A. & Aydin, A. 2004, 'A method for normalization of Schmidt hammer rebound values', *International Journal of Rock Mechanics and Mining Sciences*, vol. 41, no. 7, pp. 1211-4. DOI:10.1016/j.ijrmmms.2004.05.001
- Bellieni, G., Comin-Chiaromonte, P., Marques, L.S., Melfi, A.J., Nardy, A.J.R., Papatrechas, C., Piccirillo, E.M., Roisenberg, A. & Stofa, D. 1986, 'Petrogenetic aspects of acid and basaltic lavas from the Paraná Plateau (Brazil): Geological, mineralogical and petrochemical relationships', *Journal of Petrology*, vol. 27, no. 4, pp. 915-44, DOI:10.1093/petrology/27.4.915
- Caner, L., Radtke, L.M., Vignol-Lelarge, M.L., Inda, A.V., Bortoluzzi, E.C. & Mexias, A.S. 2014, 'Basalt and rhyodacite weathering and soil clay formation under subtropical climate in southern Brazil', *Geoderma*, vol. 235, pp. 100-12, DOI:10.1016/j.geoderma.2014.06.024
- Day, M.J. 1980, 'Rock Hardness: Field Assessment and Geomorphic importance', *The Professional Geographer*, vol. 32, no. 1, pp. 72-81, DOI:10.1111/j.0033-0124.1980.00072.x
- Dinçer, I., Acar, A., Çobanoğlu, I. & Uras, Y. 2004, 'Correlation between Schmidt hardness, uniaxial compressive strength and Young's modulus for andesites, basalts and tuffs', *Bulletin Engineering Geology and the Environment*, vol. 63, no. 2, pp.141-8, DOI:10.1007/s10064-004-0230-0
- Eppes, M.C., Magi, B., Hallet, B., Delmelle, E., Mackenzie-Helnwein, P., Warren, K. & Swami, S. 2016, 'Deciphering the role of solar-induced thermal stresses in rock weathering', *Geological Society of America Bulletin*, vol. 128, no. 9-10, pp. 1315-38, DOI:10.1130/B31422.1
- Ferrier, K.L., Huppert, K.L. & Perron, J.T. 2013, 'Climatic control of bedrock river incision', *Nature*, vol. 496, no. 7444, pp. 206-9. <https://doi.org/10.1038/nature11982>
- Flores, D.M., Lima, A.G. & Oliveira, D. 2018, 'Morfologias de leito fluvial em Riodacitos Pórfiros do Grupo Serra Geral', *Revista do Departamento de Geografia*, vol. 108, pp. 107-17, DOI:10.11606/rdg.v0ispe.144836
- Grimm, A.M., Ferraz, S.E.T. & Gomes, J. 1998, 'Precipitation Anomalies in Southern Brazil Associated with El Niño and La Niña Events', *Journal of Climate*, vol. 11, no. 11, pp. 2863-80, DOI:10.1175/1520-0442(1998)011<2863:PAISBA>2.0.CO;2
- Hancock, G.S., Anderson, R.S. & Whipple, K.X. 1998, 'Beyond power: bedrock river incision process and form', in K.J. Tinkler & E.E. Wohl (eds), *Rivers Over Rock: Fluvial Processes in*

- Bedrock Channels*, American Geophysical Union, Washington DC, pp. 35-60, DOI:10.1029/GM107
- Hancock G.S., Small E.E. & Wobus C. 2011, 'Modeling the effects of weathering on bedrock-floored channel geometry', *Journal of Geophysical Research*, vol. 116, no. F03018, DOI:10.1029/2010JF001908
- Jerram, D.A. & Widdowson, M. 2005, 'The anatomy of Continental Flood Basalt Provinces: Geological constraints on the processes and products of flood volcanism', *Lithos*, vol. 79, no. 3-4, pp. 385-405, DOI:10.1016/j.lithos.2004.09.009
- Johnson, K.N. & Finnegan, N.J. 2015, 'A lithologic control on active meandering in bedrock channels', *GSA Bulletin*, vol. 127, no. 11-2, pp. 1766-76, DOI:10.1130/B31184.1
- Langston, A. L. & Tucker, G. E. 2018, 'Developing and exploring a theory for the lateral erosion of bedrock channels for use in landscape evolution models', *Earth Surface Dynamics*, vol. 6, no. 1, pp. 1-27, DOI:10.5194/esurf-6-1-2018
- Lima, A.G. 2020, 'Mapeamento geológico da Bacia do rio das Pedras, escala 1: 30,000', in M.F. Camargo, *Diagnóstico Socioambiental da Bacia do Rio das Pedras*, Secretaria do Meio Ambiente, Prefeitura Municipal de Guarapuava. Relatório Técnico.
- Lima, A.G. & Binda, A.L. 2013, 'Lithologic and structural controls on fluvial knickzones in basalts of the Parana Basin, Brazil', *Journal of South American Earth Sciences*, vol. 48, pp. 262-70, DOI:10.1016/j.jsames.2013.10.004
- Marsh, J., Ewart, A., Milner, S., Duncan A.R. & Miller R.M. 2001, 'The Etendeka Igneous Province: magma types and their stratigraphic distribution with implications for the evolution of the Paraná-Etendeka flood basalt province', *Bulletin of Volcanology*, vol. 62, pp. 464-86, DOI:10.1007/s004450000115
- Montgomery, D. R. 2004, 'Observations on the role of lithology in strath terrace formation and bedrock channel width', *American Journal of Science*, vol. 304, no. 5, pp. 454-76, DOI:10.2475/ajs.304.5.454
- Murphy, B.P., Johnson, J.P., Gasparini, N.M. & Sklar, L.S. 2016, 'Chemical weathering as a mechanism for the climatic control of bedrock river incision', *Nature*, vol. 532, no. 7598, pp. 223-27, DOI:10.1038/nature17449
- Niedzielski, T., Migon, P. & Placek, A. 2009, 'A minimum sample size required from Schmidt hammer measurements', *Earth Surface Processes and Landforms*, vol. 34, no. 13, pp. 1713-25, DOI:10.1002/esp.1851
- Nardy, A.J.R., Machado, F.B. & Oliveira, M.A.F. 2008, 'As Rochas Vulcânicas Mesozóicas ácidas da Formação Serra Geral da Bacia do Paraná: Litoestratigrafia e Considerações Geoquímico-estratigráficas', *Revista Brasileira de Geociências*, vol. 38, no. 1, pp. 180-97.
- Paraná 1998, *Atlas de recursos hídricos do Estado do Paraná*. Suderhsa, Curitiba.
- Peate, D.W. 1997, 'The Parana-Etendeka province', *Geophysical Monograph: American Geophysical Union*, vol. 100, pp. 217-46, DOI:10.1029/GM100p0217
- Piccirillo, E.M., Comin-Chiaramonti, P., Melfi, A.J., Stolfa, D., Bellieni, G., Marques, L.S., Giaretta, A., Nardy, A.J.R., Pinese, J.P.P., Raposo, M.I.B. & Roisenberg, A. 1988, 'Petrochemistry of continental flood Basalt-Rhyolitic suites and related intrusives from the Parana Basin, Brazil', in Piccirillo, E.M. & Melfi, A.J. (eds), *The Mesozoic Flood Volcanism of the Parana Basin: Petrogenetic and Geophysical Aspects*, Instituto Geofísico, Astronômico e Ciências Atmosféricas: Universidade de São Paulo, São Paulo, pp. 107-156.
- Shobe, C.M., Hancock, G.S., Eppes, M.C. & Small, E.E. 2017, 'Field evidence for the influence of weathering on rock erodibility and channel form in bedrock rivers', *Earth Surface Processes and Landforms*, vol. 42, no. 13, pp. 1997-2012, DOI:10.1002/esp.4163
- Sklar, L.S. & Dietrich, W.E. 2001, 'Sediment and rock strength controls on river incision into bedrock', *Geology*, vol. 29, no. 12, pp. 1087-1090, DOI:10.1130/0091-7613(2001)029<1087:SA RSCO>2.0.CO;2
- Small E.E., Blom T., Hancock G.S., Hynke B. M. & Wobus C.W. 2015, 'Variability of rock erodibility in bedrock-floored stream channels based on abrasion mill experiments', *Journal of Geophysical Research, Earth Surface*, vol. 120, no. 8, pp. 1455-1469, DOI:10.1002/2015JF003506
- Stock, J.D., Montgomery, D.R., Collins, B.D., Dietrich, W.E. & Sklar, L. 2005, 'Field measurements of incision rates following bedrock exposure: Implications for process controls on the long profiles of valleys cut by rivers and debris flows', *Geological Society of America Bulletin*, vol. 117, no. 1-2, pp. 174-194, DOI:10.1130/B25560.1
- Sumner, P. & Nel, W. 2002, 'The effect of rock moisture on Schmidt hammer rebound: tests on rock samples from Marion Island and South Africa', *Earth Surface Processes and Landforms*, vol. 27, no. 10, pp. 1137-1142, DOI:10.1002/esp.402
- Thomaz, E.L. & Vestena, L.R. 2003, *Aspectos climáticos de Guarapuava – PR*, Unicentro, Guarapuava, 106 p.
- Truffi, S.A. & Clemente, C.A. 2002, 'Alteração de plagioclásios dos riodacitos da Formação Serra Geral (JKsg) da região de Piraju-SP', *Scientia Agricola*, vol. 59, no. 2, pp. 383-388, DOI:10.1590/S0103-90162002000200026
- Turner, S.P., Regelous, M., Kelley, S., Hawkesworth, C.J. & Mantovani, M.S.M. 1994, 'Magmatism and continental break-up in the South Atlantic: high precision 40Ar-39Ar geochronology', *Earth and Planetary Science Letters*, vol. 121, no. 3-4, pp. 333-348, DOI:10.1016/0012-821X(94)90076-0
- Yagiz, S. 2009, 'Predicting uniaxial compressive strength, modulus of elasticity and index properties of rocks using the Schmidt hammer', *Bulletin of Engineering Geology and the Environment*, vol. 68, no. 1, pp. 55-63, DOI:10.1007/s10064-008-0172-z
- Whipple, K.X., Hancock, G.S. & Anderson, R.S. 2000, 'River incision into bedrock: mechanics and relative efficacy of plucking, abrasion, and cavitation', *Geological Society of America Bulletin*, vol. 112, no. 3, pp. 490-503, DOI:10.1130/0016-7606(2000)112<490:RIIBMA>2.0.CO;2

- Whipple, K.X., DiBiase, R.A. & Crosby, B.T. 2013, 'Bedrock rivers', in J. Shroder & E. Wohl (eds), *Fluvial Geomorphology: Treatise on Geomorphology*, Elsevier, vol. 9, pp. 550-573.
- Whittaker, A. C., Cowie, P. A., Attal, M., Tucker, G. E. & Roberts, G. P. 2007, 'Bedrock channel adjustment to tectonic forcing: Implications for predicting river incision rates', *Geology*, vol. 35, no. 2, pp. 103-6, DOI:10.1130/G23106A.1
- Wohl, E.E. 1998, 'Bedrock channel morphology in relation to erosional processes', in K.J. Tinkler & E.E. Wohl (eds), *Rivers over Rock: Fluvial Processes in Bedrock Channels*, American Geophysical Union, Washington, DC, pp. 133-51, DOI:10.1029/GM107

**Author contributions**

**Adalto Gonçalves Lima:** conceptualization; methodology; formal analysis; writing-original draft; writing – review and editing; visualization. **Ana Carolina Carvalho Galvão:** formal analysis; investigation; visualization. **Diego Moraes Flores:** methodology; writing-original draft; visualization.

**Conflict of interest**

The authors declare no conflict of interest.

**Data availability statement**

Data are available on request.

**How to cite:**

Lima, A.G., Galvão, A.C.C., & Flores, D.M. 2024, 'Weathering and River Erosion: Insights from the Variation of Intact Rock Strength in Rhyodacites', *Anuário do Instituto de Geociências*, 47:49202. [https://doi.org/10.11137/1982-3908\\_2024\\_47\\_49202](https://doi.org/10.11137/1982-3908_2024_47_49202)

**Funding information**

Not applicable

**Editor-in-chief**

Dr. Claudine Dereczynski

**Associate Editor**

Dr. Márcio Fernandes Leão